Application of the ultrasound velocity measuring technique to stirred vessel flows

P. Wächter, W. Steidl, M. Höfken, F. Durst

performed at the

Institute of Fluid Mechanics of the Friedrich-Alexander-University Erlangen-Nuremberg

P. Wächter, W. Steidl[1], F. Durst

Lehrstuhl für Strömungsmechanik, Friedrich-Alexander-Universtät Erlangen-Nürnberg

Cauerstraße 4, D-91058 Erlangen, Germany

Correspondence to: P. Wächter

[1] *Present address*: Invent Umwelt- und Verfahrenstechnik GmbH & Co. KG,

Am Weichselgarten 7, D-91058 Erlangen, Germany

M. Höfken

Invent Umwelt- und Verfahrenstechnik GmbH & Co. KG,

Am Weichselgarten 7, D-91058 Erlangen, Germany

Abstract This publication presents results of local velocity measurements in a stirred vessel obtained by means of ultrasound Doppler anemometry. The flow in a rectangular tank, equipped with a hyperboloid stirrer, was investigated with respect to the mean flow field, the

mean turbulence properties and the avarage characteristic length scales of turbulence. The ultrasound Doppler anemometry was utilized to demonstrate its applicability to stirred vessel flows. The employment of this technique in the present work demonstrates its ease of use. Since the measurements result in velocity profiles rather than point measurements, the relevant velocity information could be obtained in short times.

Symbols

c	Sound velocity	m/s
C	Constant value in equation (9)	-
d_R	Stirrer diameter	m
f_0	Basic frequency of the UVP-monitor	s^{-1}
f_d	Doppler frequency	s^{-1}
f_{prf}	Pulse repetition frequency	s^{-1}
L	Ultrasound beam length	m
L	Macro value of turbulent flow	m
L_I	Integral length value in stirred systems	m
n	Revolutions per second	s^{-1}
N	Number of measuring points	-
Ne	Newton number	-
P	Power input of the stirrer	J/s
Re	Reynolds number	-
t_I	Integral time value	-
Tu	Degree of turbulence	-
U	Mean velocity	m/s
U_{Tip}	Circumferential velocity of the stirrer	m/s
u'	Rms-value of turbulent velocity fluctuations	m/s
V	Volume	m^3
z	Size of confidence interval	-
ε	Statistical error	-
ε_{ges}	Total specific power intake	m^2/s^3
ε_{loc}	Local energy dissipation	m^2/s^3
η	Kolmogorov microscale	m

λ	Taylor microscale	m
ν	Kinematic viscosity	m^2/s
ρ	Fluid density	kg/m^3
σ_x^2	Standard deviation	-
Λ	Macroscale of turbulence in stirred systems	m
Ω	Sampling rate	s^{-1}

1

Introduction

Stirred flow reactors are widely employed in process engineering with applications ranging from maintaining suspensions, production of emulsions through to improvements of mixing and enhancement of heat transfer. Convential design methods for stirred flow reactors employ integral information such as input energy, mixing time, etc. and scale-up rules to predict the performance of large stirrers from small scale experiments. It is only recently that advancements in numerical techniques and the increase in available computer power permit numerical predictions of stirred vessel flows. Such computer codes solve the time averaged Navier-Stokes equations (Reynolds equations), extended by turbulence models to close the resulting set of partial differential equations. The solutions of these equations provide local information on time averaged mean flow and turbulence properties. In the case of predictions of stirred vessel flows, local turbulence information results (see e.g. Kresta and Wood (1992), Yianneskis et. al. (1987, 1993, 1994), Höfken (1994)), which can extend empirical correlations of stirred vessel flows, e.g. as provided by Nicolaus (1961). However, the turbulence models employed for numerically predicting the flow, contain model assumptions, which need to be experimentally verified in stirred vessel flows.

To investigate the velocity field of stirred vessel flows, a multi-purpose mixer test facility has been designed, manufactured and put into service at *LSTM*-Erlangen. It is equipped with

an ultrasound Doppler anemometer and features also a flow visualisation facility employing the laser light sheet technique. The test rig can be used to experimentally study various stirrers in detail and to carry out flowvelocity measurements to obtain a database for the validation of numerical simulations. It is demonstrated in this paper that the ultrasound Doppler technique is suitable for obtaining detailed and comprehensive experimental velocity profile data in stirred vessel flows.

The ultrasound Doppler technique, as it stands today, can not compete with laser Doppler anemometery with respect to the spatial resolution of the measurements, but the technique shows a variety of other advantages that makes it interesting to stirred vessel flows. No optical access to the measuring volume is necessary and so the probe can be set outside an optically non-transparent wall. It also can be applied to opaque fluid flows. Furthermore, the employment in tanks of an industrial scale is possible because the available ultrasound probes are water resistant and can be immersed in most measuring fluids. An ultrasound Doppler anemometer can also obtain a complete velocity profile over the penetration length of the ultrasound beam which helps to reduce the measurement time.

The present paper is written to document the authors' investigation of stirred vessel flows with the METFLOW S.A. UVP-Monitor, a commercially available ultrasound Doppler velocimeter. In chapter 2 the test facility, the water tank and the stirrer that were used are explained. Chapter 3 deals with some basic information about ultrasound Doppler anemometry, the accuracy of the measurements, and the evaluation of the data by special software. The results of the investigations, i.e. the flow field and the turbulent properties, are shown in Chapter 4. This paper will close with some conclusions derived from the presented results.

2

Test facility and stirrer

In recent years laser Doppler anemometry has proven to be the most precise and reliable measuring technique for highly turbulent flows which occur in stirred vessels, more accurate than other techniques such as Pitot probes and hot wire anemometers. But a standard LDA system results only in flow information at a single measuring point, i.e. time traces of a local velocity. This is disadvantageous where velocity information is needed in the entire flow field. For this purpose, the LDA-measuring volume needs to be traversed and the resultant flow field information is provided by a sequence of point measurements. This is time consuming. It is therefore desirable to use techniques that provide "profile information", rather than "point information" of the velocity field. The ultrasound Doppler velocimeter is a technique of this kind, providing in a short time the entire velocity profile along the ultrasound beam. Hence, the application of this technique to stirred vessel flows should result in shorter measuring times, but might result in velocity information of less temporal and spatial resolution.

To demonstrate the applicability of the ultrasound Doppler technique in stirred vessel flow and quantify its resolution, the present study was performed. A multi-functional test rig for stirred vessel flow investigations was set up at *LSTM*-Erlangen and equipped with laser light sheet optics to permit flow visualization of the overall flow field in the rectangular water tank. A sketch of the test facility is given in Figure 1, showing the main components of the tank, the light sheet glass fibre optics and the Ultrasound Velocity Profile (UVP) Monitor X-1.

2.1

The water tank

The internal dimensions of the experimental vessel were 1,750 mm x 400 mm x 550 mm. The Plexiglas vessel had a wall thickness of 25 mm. It was seperated into two sections by a dividing wall, which could be set to any desired position, so that practically any rectangular vessel geometry could be achieved. The tank was constructed in such a way to have the opportunity of studying different tank geometries, as they are used in waste water treatment plants, but at a model scale. With this test rig it is possible to determine the necessary rotational speed of stirrers to fulfil a desired mixing task, e.g. to keep particles homogeneously suspended. Furthermore, it is possible to determine the number of stirrers which should be employed in a longitudinal tank with respect to the investment and the running costs. In the present investigation a square vessel of dimensions (T x T x H) 400 mm x 400 mm x 500 mm was chosen.

On one longitudinal and one lateral side of the vessel, aluminium rails were mounted above and below, that allowed the mounting of brackets to hold the UVP transducer and to traverse it to every required position.

The x, y and z components of the velocity vectors were determined in nine horizontal measurement planes of 8 x 8 measuring points. The locations of the individual measuring points can be seen from Figure 2 below. The coordinates of the measuring points on each axis were set as follows in Table 1.

The front left-hand corner of the experimental vessel was chosen as the coordinate origin. The x-axis ran along the length of the vessel and the y-axis represented the width. Due to symmetry, only one quarter of the vessel was measured. For the evaluation it was possible to apply these measured data to the entire vessel.

2.2

Stirring technique

A hyperboloid stirrer of the diameter D= T/4= 100 mm (Figure 3) was used in the experiments. The stirrer body, milled out of brass, was mounted on a steel shaft centered in the vessel. The clearence to the vessel's bottom was C= D/10= 10 mm. This stirring element is mainly used to suspend particles, where most of the energy brought into the fluid is needed to remove solids from the bottom. Therefore the above mentioned ratios with the comparatively low clearence proved to be very effective, because the energy is input into the part of the tank where it is required. The induced flow remains attached to the upper surface of the stirrer body. Hence, separation and resulting energy losses are minimized. The stirrer body was equipped with 8 transport ribs, which protrude 2 mm from the surface of the stirrer.

The required stirrer speed was set through the output voltage of the power supply (Gossen, SSP-Konstanter 62 N). This value was monitored by an encoder on the shaft of the electric motor Type E644 of the Electro Craft Cooperation.

A constant stirrer speed of 573 rpm was used for the measurements, which corresponds to a circumferential tip speed of 3 m/s. A Reynolds number of 95,500 was achieved by using water as test fluid. This velocity has shown to be sufficient to remove sludge from the bottom of the tank and to keep it suspended. This system has proven to be suitable for simulating the flow field of activated sludge basins in waste water treatment plants.

3

The ultrasound Doppler anemometry

Detailed characterization of the stirrer/stirred vessel system requires explicit knowledge of the mean and the turbulent flow field in the stirred vessel. This places high demands on the accuracy of the measuring system.

Similar to laser Doppler anemometry, the ultrasound Doppler anemometer, measures the local velocity by determining the Doppler shift caused by slip-free particles in the fluid. In contrast to LDA methods however, by using different time windows, measurements can be taken at several successive points along the ultrasound beam. The ultrasound signals are transmitted by a transducer and received again after reflection from the scattered particles. This measuring principle of ultrasound Doppler anemometry is shown schematically in Figure 4.

3.1 Basic principles of the ultrasound Doppler anemometry

In the following some fundamental background of the ultrasound Doppler anemometry is given, in particular, that there is a limitation in the maximum measureable velocity and the penetration length, which is inherent to the measurement technique. Other effects like the absorption of the ultrasound in solids and fluids, which also reduce the penetration of the beam and lead to a decreasing signal to noise ratio, are not discussed here.

The Doppler shift f_d is directly related to the velocity component U of the respective scattered particle, which is aligned with the beam propagation direction. The flow velocity can be determined without the need for further calibration of the measuring instrument, provided the velocity of sound in the fluid is known.

$$U = c \cdot \frac{f_d}{2 \cdot f_0} \qquad (1)$$

The measuring beam is effectively subdivided into successive measuring points by way of the fact that the device measures the Doppler shift frequency at different time instances following transmission of the ultrasound signal. The maximum penetration depth, i.e. the maximum measuring length over which a total velocity profile can be acquired is limited by the pulse repetition frequency f_{prf} and the signal to noise ratio:

$$L_{max} = \frac{c}{2 \cdot f_{prf}} \tag{2}$$

To obtain a single profile, 128 pulses are provided and evaluated for each measuring point. In order to fulfil the Nyquist sampling criterion for determining the Doppler frequency, which is done by a Fourier analysis, at least two pulses are required per period. For the maximum detectable Doppler frequency

$$f_{D_{max}} < \frac{f_{prf}}{2} \tag{3}$$

applies and therefore also the maximum measurable velocity is dependent on the pulse repetition frequency

$$U_{max} < \frac{c \cdot f_{prf}}{4 f_0} \quad . \tag{4}$$

A common criterion is therefore obtained which demonstrates the dependence of the maximum measurable velocity on the measuring length:

$$L_{max} \cdot U_{max} < \frac{c^2}{8 \cdot f_0} \tag{5}$$

This shows that large penetration depths can only be obtained at the cost of the maximum measurable velocity.

3.2

Analysis of the accuracy of UVP measurements

Statistical independence

In the case of measurements in turbulent flow, it is extremely important to ensure the statistical independence of the measured values, otherwise errors can occur in the calculation of average values and the turbulent fluctuations (rms value). The statistical independence is checked, according to Tropea (1993), using the integral time scale of the typical large-scale flow variations. For the fluid mechanics problem under investigation here, a characteristic length of L_1 = 100 mm corresponding to the diameter of the stirrer element used and a characteristic speed of U_{Tip} = 3 m/s corresponding to the circumferential tip speed of the hyperboloid stirrer were assumed. The integral time scale is therefore obtained as follows:

$$t_1 = \frac{L_1}{U_{Tip}} = \frac{0{,}1 \ \ [m]}{3{,}0 \ \ [m/s]} = 0{,}033 \ \ [s] \tag{6}$$

The integral time scale has the following characteristics:

- Signals at intervals of 2 t_I contribute to the average value as a single, statistically independent measured value.
- Signal values only become statistically independent when a period of 2 t_I lies between them.

The maximum sampling rate Ω, at which statistically independent velocity values are acquired, is obtained from these conditions as

$$\Omega = \frac{1}{2 \cdot t_I} = 15 \quad [\text{Hz}] \quad . \tag{7}$$

The time resolution of the measurements, calculated using the pulse repetition frequency for the 128 pulses, is 65,5 ms for the selected penetration length. For realizing a real-time data analysis, the time interval between two measurements is 69.8 ms or 14.3 Hz respectively. If this value is compared with the maximum sampling rate Ω, it becomes apparent that the velocity values obtained are statistically independent.

Statistical error

The following equation applies for the statistical error in the velocity measurement, according to Tropea (1993):

$$\varepsilon = \sqrt{\frac{z^2 \cdot \sigma_x^2}{N}} \tag{4}$$

This includes the standard deviation σ_x^2, which is obtained from the rms value; the number of measuring points N; and a factor z that characterizes the size of the confidence interval. With a confidence interval of 96 %, i.e. for z = 2 and an rms value measured in close proximity of the stirrer of 150 mm/s, the statistical error ε is specified in Table 2 for different values of N. For the relative error with respect to the maximum measurable velocity value (which was 181 [mm/s] in the measurement mentioned above, in close proximity of the stirrer), the relationship to N is given in Table 3.

3.3

Evaluation software

A flow chart of the evaluation procedure is shown in Figure 5, naming also the programmes used. The programmes printed in italics were developed specifically at the Department of Fluid Mechanics for the 3-dimensional presentation of results. This was necessary to obtain a graphical representation that allows a comprehensive insight into the fluid flow.

The programme *uvpgraph* allowed a fast evaluation of the binary data obtained by the Ultrasound Velocity Profile Monitor. The velocity and the rms value were calculated for every measuring point. It took into consideration that the sound veloctity in the wall differed from that in the fluid. The programme *quad2tec* had mainly the task to provide the data format which was needed for TECPLOT, a commercial software of Amtec Engineering, Inc., to visualize data records.

4

Results of the ultrasound Doppler measurements

With the ultrasound velocity technique, described in section 3, the entire velocity field was mapped out. To obtain the result that were presented in the following, a total of 2,200 separate profiles were recorded which involved a measuring time of 55 hours. From these separate profiles, 208 average velocity profiles were then calculated from which the relevant velocity components could be correlated to the 576 individual measuring points.

4.1

Graphical presentation of the flow field

The results measured with the UVP monitor were subdivided into different horizontal and vertical planes that could be displayed individually using the commercial post-processing software TECPLOT.

The velocity field for the flow was described on the one hand using vectors for a clear picture of the flow direction. On the other hand, the values of absolute velocity with respect to the circumferential speed of the stirrer were presented as coloured contoured surfaces that provide an overview of the global velocity distribution. When the fluid velocity relative to the stirrer circumferential speed are plotted, the velocity distribution for the measured geometric form is obtained independently of the stirrer speed. In highly turbulent stirred flows the average velocity and the turbulent fluctuations are directly proportional to the stirrer speed, so this allows the absolute velocities to be determined for any rotational speed in the area of turbulence. In addition, the values for the relative fractions of velocity components with respect to the absolute velocity was displayed as a coloured contoured surface in order to restore the velocity impression in the depth of a plane that had been lost in the two-dimensional vector representation of the plane.

A presentation in the form of coloured contours was also used for evaluating the local energy dissipation because this variable is a scalar and has no direction and cannot therefore be displayed in vector form.

The results for the horizontal planes are depicted on the following pages. It can be seen from the *vector presentation* (Figure 6) of the floor level that the stirrer drives the fluid right into the corners at a relatively high velocity whereby with careful design the deposit of solids in the corners can be prevented. If this corner flow is traced further in the subsequent plane, it is illustrated that a flow forms close to the wall that runs in the opposite direction to the main flow. This flow arose due to the strong axial flow in the corners following diversion of the floor flow to the vertical. With increasing height, this effect loses significance and the flow gradually transforms into a rotational flow about the stirrer axis. In planes z = 164 to z = 346, the horizontal projection of a vortex with the stirrer shaft at its centre is shown.

From a glance at the presentation of the *relative axial velocity* (Figure 7), in the central planes, the areas of increased axial flow can be seen clearly that form around the stirrer shaft. In these areas, the fluid was flowing back towards the stirrer. The other significant areas with a high axial flow component are the corners. These high relative velocities in the corners are found as far up as the upper planes; so even in the case of tall vessels, the hyperboloid stirrer can provide good stirring effects.

The graph of *relative velocity* (Figure 8) in the various horizontal levels shows that at a height of 34 mm, i.e. only 26 mm from the floor level, the flow velocity became significantly smaller. From the velocity distribution in the planes z = 34 mm and z = 60 mm, the areas of increased velocity at the edge of the vessel and in close proximity of the stirrer can be clearly distinguished. The high velocity at the wall was a result of the change in direction of the floor flow to the vertical. In the plane z = 60 mm, velocities of 0.03 x U_{tip}, i.e. 9 cm/s, were reached

here. The area of increased velocity around the stirrer was due to the return flow of the fluid driven upwards at the wall towards the stirrer. This is particularly clear in the presentation of *relative axial velocity* (Figure 7). In the planes z = 112 mm and z = 164 mm in Figure 7, the relatively low flow velocities in the two preceding lower planes are no longer present. These zones visible in form of dark blue coloured regions in the two lower planes presumably represent the vortex centres of the large scale vortex that forms in the lower corners. An evaluation of the vector presentation of the flow velocity for the vertical levels produced the value of approximately 70 mm for the horizontal distance of the vortex centre from the floor. In the subsequent planes, z = 216 mm and z = 268 mm, the high velocities at sections of the vessel wall can be detected again.

Whereas in the lower planes, these velocity peaks arose in a strip parallel to the x-axis, they were now found in an area parallel to the y-axis. The reason for this was presumably the upwards flow close to the wall overlapping with the clockwise rotating flow around the stirrer. This caused the velocity peak to move slowly in the direction of rotation of the stirrer. In the top two planes, z = 346 mm and z = 424 mm, the measured velocities had already fallen to a fifth of the maximum floor velocity. On the whole, in these planes, the measured velocities were distributed quite evenly over the entire plane.

The graph of the *turbulent velocity field* in the vertical direction (Figure 9) represents planes in a side view. In the plane y =7 mm, which shows the detail next to the wall, it can be seen clearly how the fluid was moved along the corners up to the surface. This upwards directed flow is along the whole wall visible even if it is not so marked in the heights of 346 mm and 424 mm. In a distance of 57 mm of the wall the above described ring vortex was formed in the lower left and right part of the vessel. These structures were becoming clearer and clearer with looking at the sequence of planes. The plane y =197 mm is nearly an intersection with the

stirrer shaft where the flow streams downwards along the shaft to be moved along the vessel's bottom to the wall and then again upwards to the surface. Because the coordinate y =200 mm is the middle of the tank the vector field is nearly symmetrical relating to the shaft.

From the presentation of the *local energy dissipation* (Fig. 10) it is clear that the largest portion of the input energy was concentrated in a ring-shaped area around the stirrer in the floor area. In the other areas, the energy input was significantly lower and remained practically constant over the entire height of the vessel. In the central planes, a value of around 1.0 was obtained for the local energy dissipation, i.e. the average energy component falling on this partial volume was transferred in its entirety, whereas in the upper levels the local energy input fell slightly as expected.

4.2

Interpretation of the results

The results show the applicability of the ultrasound Doppler anemometry to stirred vessel flows. The large-scale flow patterns generated by the hyperboloid stirrer were detected very well. Nevertheless there are some limitations, which restrict the obtainable information.

In the immediate vicinity of the stirrer, acoustic reflections of the stirrer and its shaft complicate the evaluation and interpretation of the signals. Also important to point out is the spatial resolution, which is given by the beam diameter, of more than 4 mm. As an example, the effect is shown in comparison with laser Doppler measurements in Figure 11. It concerns an angle-resolved measurement, which allows to take the periodic variations produced by the blades of the stirrer into account.

The intersection of the beams and hence the two dimensional plane of the measuring volume of the ultrasound Doppler measurements is marked. This graph explains why the

measuring points next to the stirrer in Figures 6 and 9 must not show the highest velocities. The vector presentation of the laser Doppler measurements makes clear that the fluid moves downwards before reaching the measuring volume of the ultrasonic Doppler measurement. Then the fluid flows along the bottom in the radial direction and spreads in a way, so that the high velocity is detected in the following measuring volume.

4.3

Determining the turbulence variables

The local energy dissipation in a stirred vessel can be determined via the constant C that takes on a characteristic value for the stirrer/stirred vessel system as follows Brodkey (1975):

$$\varepsilon_{loc} = C\frac{u_i'^3}{d_R} \tag{5}$$

Where the constant C can be calculated from the volume-related variation velocities :

$$C = \frac{\overline{\varepsilon_{ges}}}{\sum \frac{u_i'^3}{d_R}} \tag{6}$$

$$\sum u_i'^3 = \frac{\sum V_i u_i'^3}{V_{ges}} \tag{7}$$

The average power input $\overline{\varepsilon_{ges}}$ with respect to the mass inside the stirred vessel, can be obtained via the Newton number Ne of the stirrer element :

$$\overline{\varepsilon_{ges}} = \frac{P}{\rho V} = \frac{Ne \cdot n^3 \cdot d_R^5}{V} \tag{8}$$

It is also of interest to determine the microscales, that describe the smallest vortex that occurs in a turbulent flow, which are independent of the geometric size of the experimental set-up. The so-called Kolmogorov and Taylor microscales are commonly used here Landahl et al. (1986):

$$\eta = \left(\frac{\nu^3}{\varepsilon}\right)^{\frac{1}{4}} \quad \text{(Kolmogorov)} \tag{9}$$

$$\lambda^2 = \frac{\overline{u'^2}}{\left(\frac{\partial u'}{\partial x}\right)^2} \quad \text{(Taylor)} \tag{10}$$

The following approximate relationship exists between these two length values:

$$\frac{\lambda}{\eta} = Re^{\frac{1}{4}} \tag{11}$$

As can be seen from the above equation [15], as the Reynolds number of the flow increases, the difference between the two values also increases.

Assuming that the macro scale L for the turbulent stirrer flow corresponds to the stirrer diameter d_R, the turbulence values of Table 4 were obtained.

By setting C to "1" in the equation for determining the constant C, a characteristic length value of L = 6.7 mm is obtained, which corresponds to about a fifteenth of the stirrer diameter. The macro scale Λ for the largest vortex can be determined from this characteristic length using the formula from Brodkey

$$\Lambda = \frac{3}{8} \cdot L. \tag{12}$$

This gives a value of Λ = 2.18 mm which corresponds to the rib height of 2 mm to an acceptable degree of accuracy.

5

Conclusions

This investigation shows that the ultrasound Doppler anemometry is a useful technique for examining large-scale flows in model tank reactors. Because of the spatial resolution this technique is predestined for characterizing flows where no detailed information in the nearer vicinity of the stirrer are needed, e.g. for multi-stirrer configurations or stirrer flows with a superimposed in- and outflow.

Nevertheless, the most important goal of the investigations described above, to gain more knowledge about the turbulent large scale flow field induced by a hyperboloid stirrer, was attained. All the data gathered will help to improve the design of hyperboloid stirrers. Measuring the turbulent fluctuation velocities, it should now be possible to calculate the mass and heat transfer rates with higher accuracy. The acquired Kolmogorov micro scales allow the prediction of the minimum particle size that can be suspended by the hyperboloid stirring

system, Herdel (1982) and Höfken (1994). The obtained data will also be very useful to validate CFD-simulations.

References

Brodkey, R. S. : *Turbulence in Mixing Operations*, Academic Press, New York, 1975

Herndl, G. : *Stoffübergang in gerührten Suspensionen*, Dissertation, München, 1982

Höfken, M. : *Moderne experimentelle Methoden für die Untersuchung von Strömungen in Rührbehältern und für Rührwerksoptimierung*, Dissertation, Erlangen, 1994

Landahl, M., Mollo-Christensen, E. : *Turbulence and random processes in fluid mechanics*, Cambridge University Press, Cambridge, 1986

Kresta, S. M., Wood, P. E.: *The Flow-field Produced by a Pitched Blade Turbine: Characterization of the Turbulence and Estimation of the Dissipation Rate*, Chem. Eng. Sci., vol. 48, pp. 1761-1774, 1992.

Nicolaus, F. : *Suspendieren von Festkörpern in Flüssigkeiten durch Rührer*, Dissertation, München, 1961

Tropea, C. : *Statistische Ermittlung strömungsmechanischer Größen*, Vortrag auf dem Kurzlehrgang „Präzisions-Messungen mittels Laser-Doppler-Anemometrie und Phasen-Doppler-Anemometrie", Erlangen, 1993

Yianneskis, M, Popiolek, Z., Whitelaw J. H., *An Experimental Study of the Steady and Unsteady Flow Characteristics of Stirred Reactors,* J. Fluid Mech., vol. 175, pp. 537-555, 1987.

Yianneskis, M., Whitelaw, J. H., *On the Structure of the Trailing Vortices around Rushton Turbine Blades,* Trans. IChemE, vol. 71, Part A, pp. 543-550, 1993.

Yianneskis, M., Rutherford, K., Lee, K. C., *The Interaction of the Trailing Vortex Streams from Rushton Turbine Blades,* Seventh International Symposium on Applications of Laser Techniques to Fluid Mechanics, Lisbon, vol. 1, pp. 10.2.1-10.2.7, 1994.

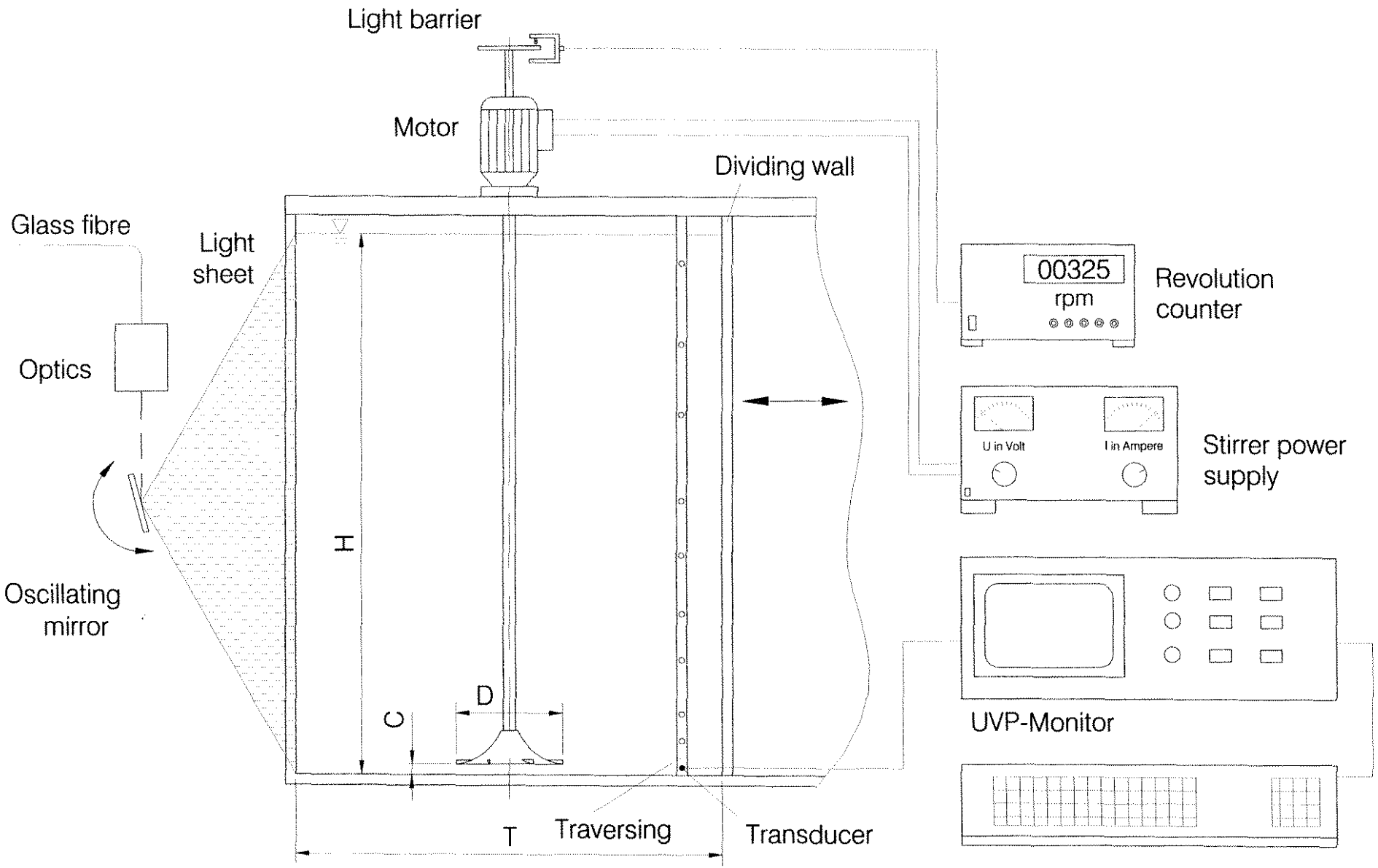

Fig. 1: Experimental set-up

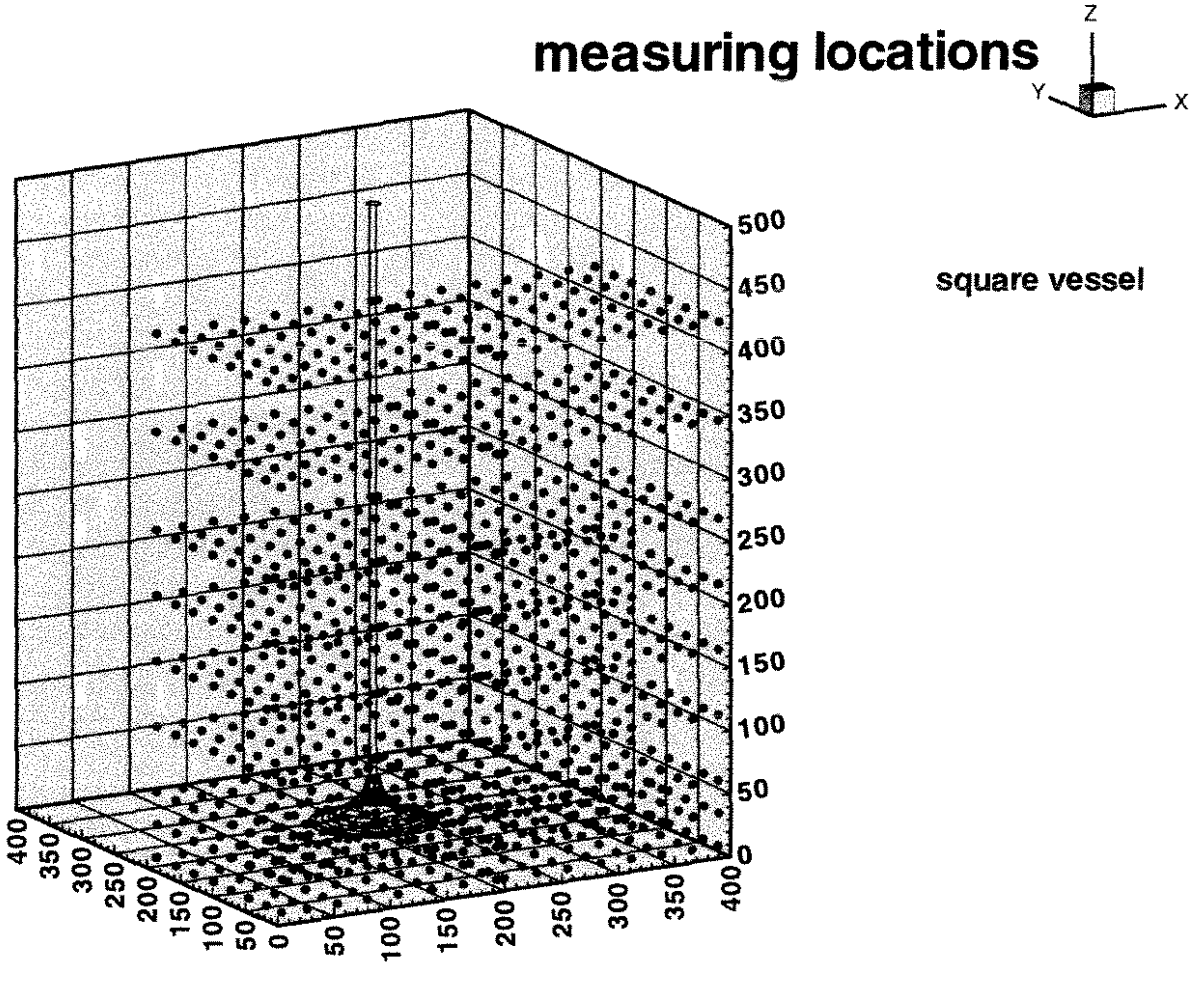

Fig. 2: Locations of the measuring points in the quadratic vessel

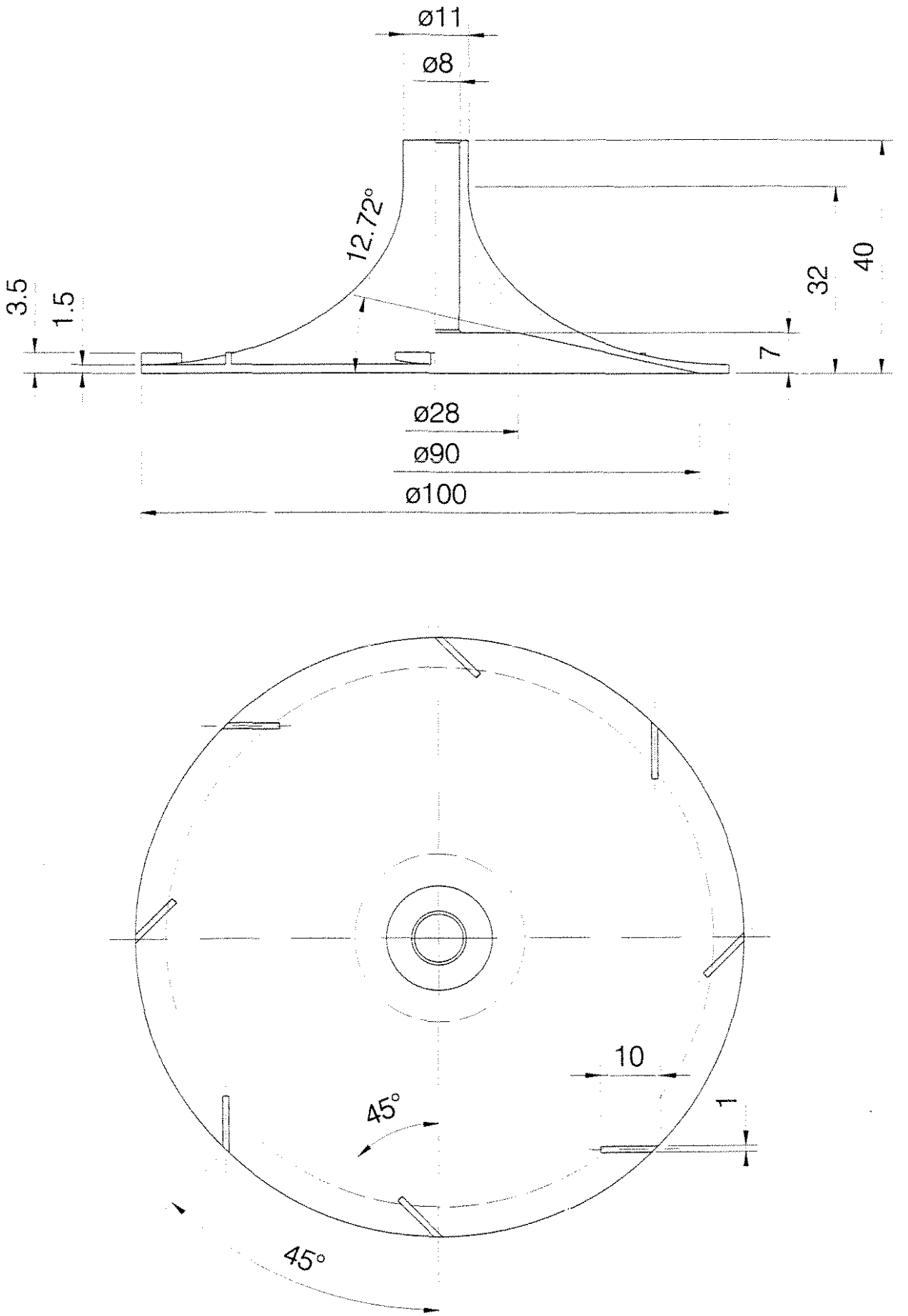

Fig. 3: Hyperboloid stirrer used

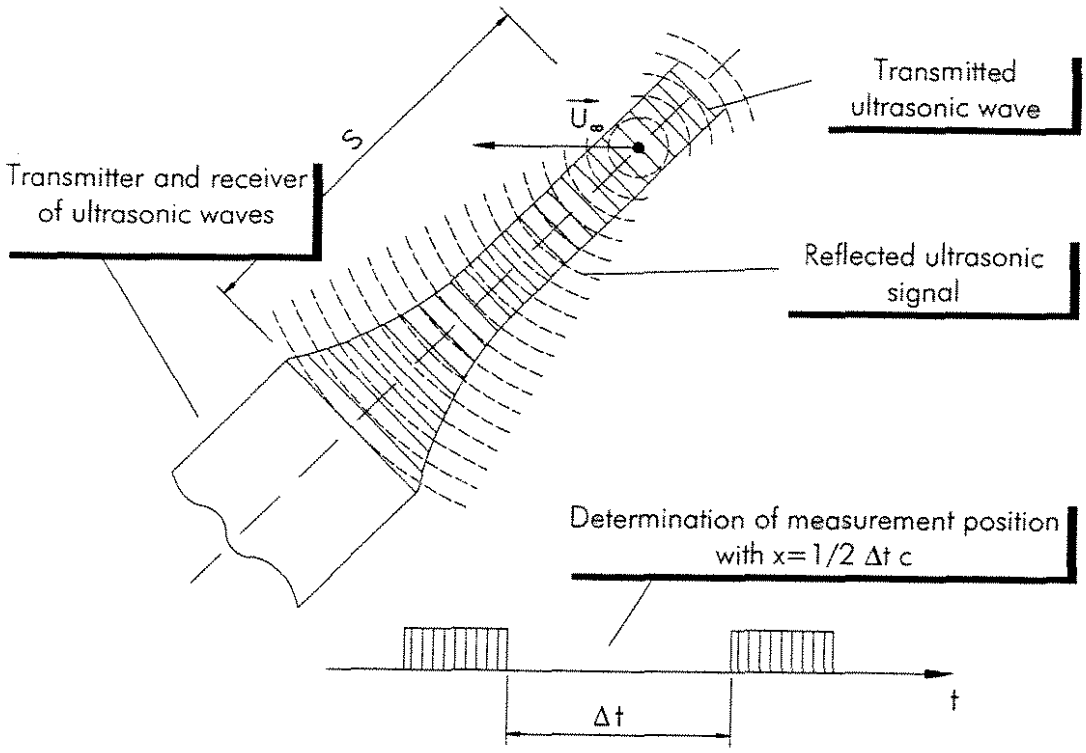

Fig. 4: Measuring principle of ultrasound Doppler anemometry

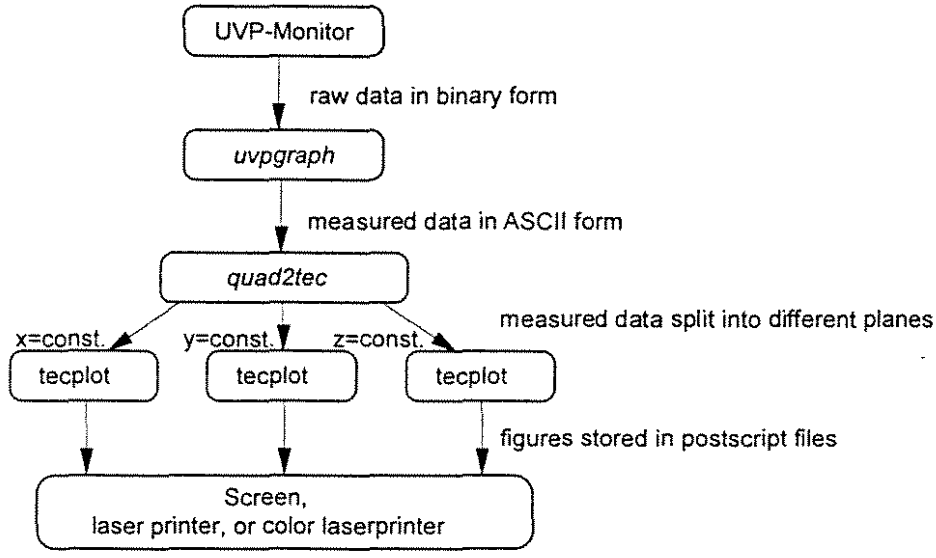

Fig. 5: The evaluation procedure from measured data acquisition to the printout

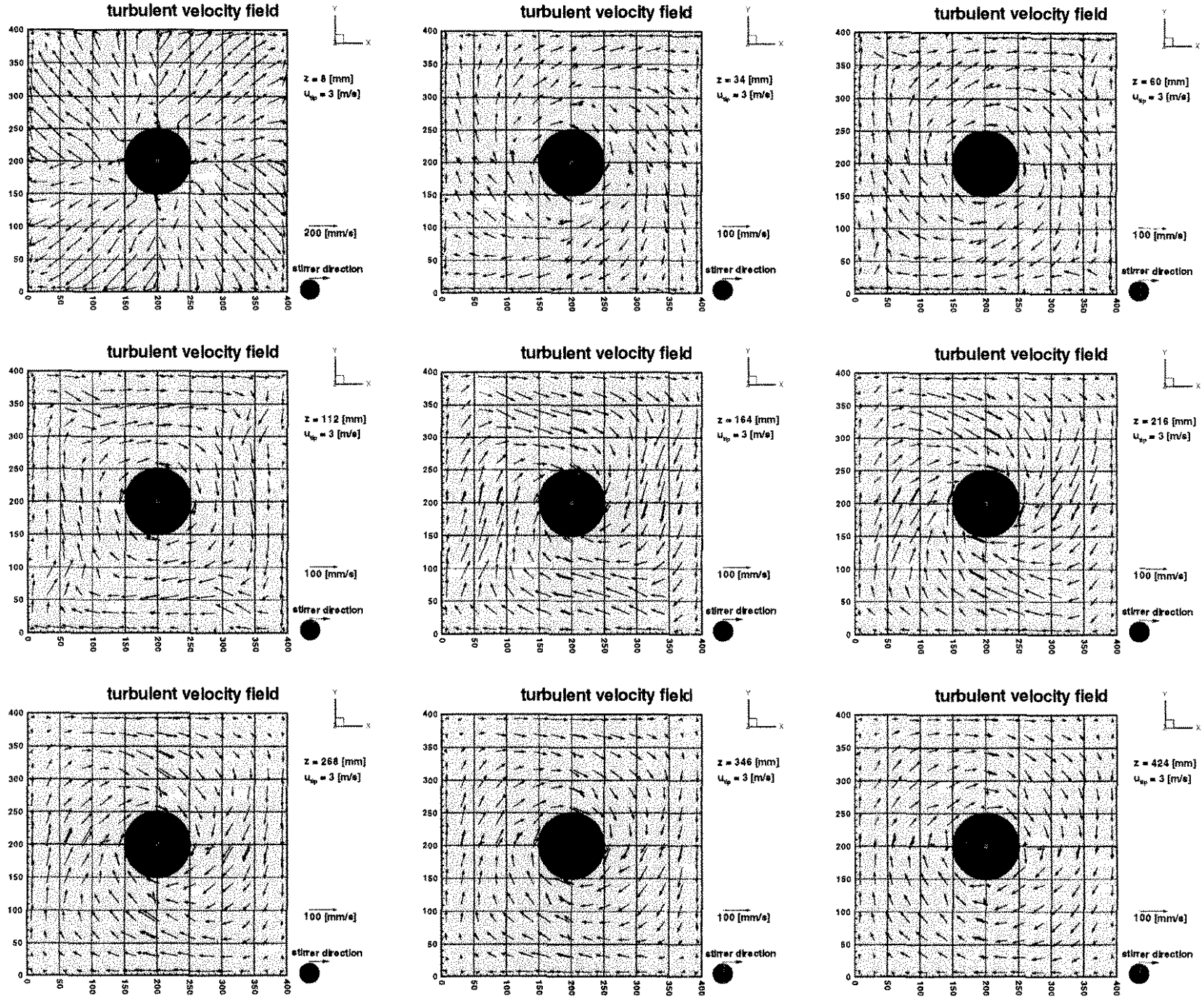

Fig. 6: Presentation of the vector field of velocity for the horizontal planes

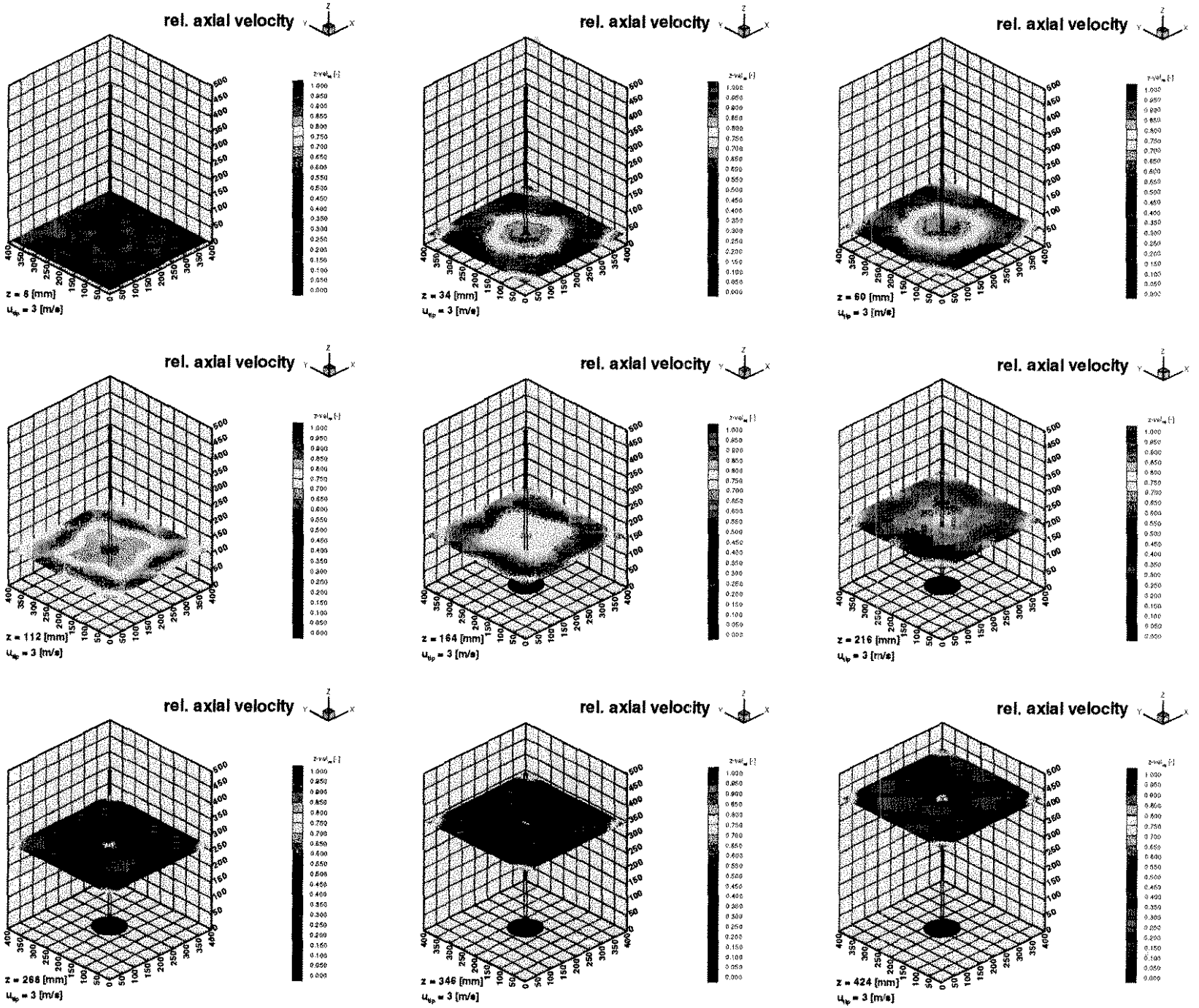

Fig. 7: Presentation of the relative axial velocity for the horizontal planes

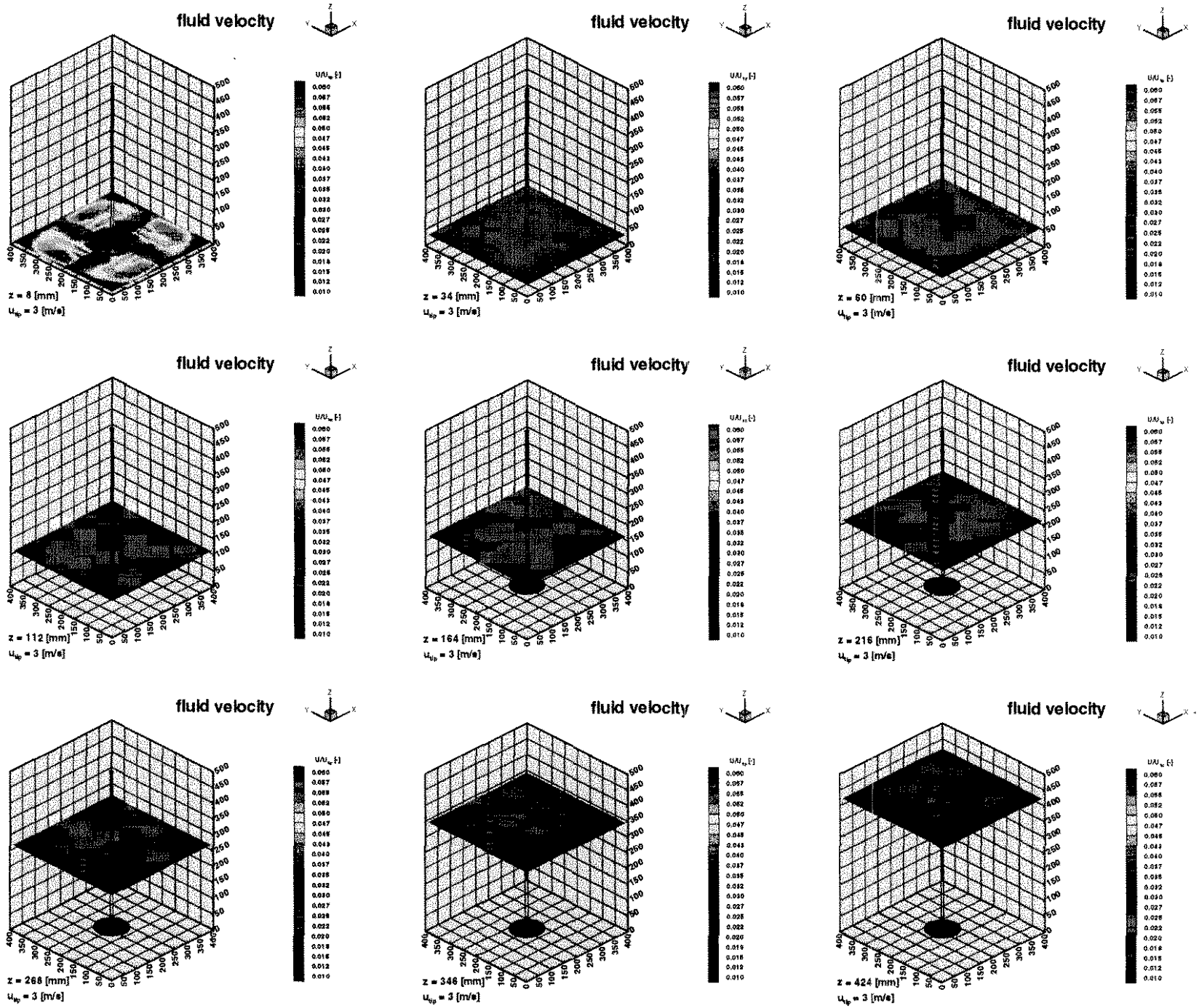

Fig. 8: Presentation of the nondimensional velocity U/U_{Tip} for the horizontal planes

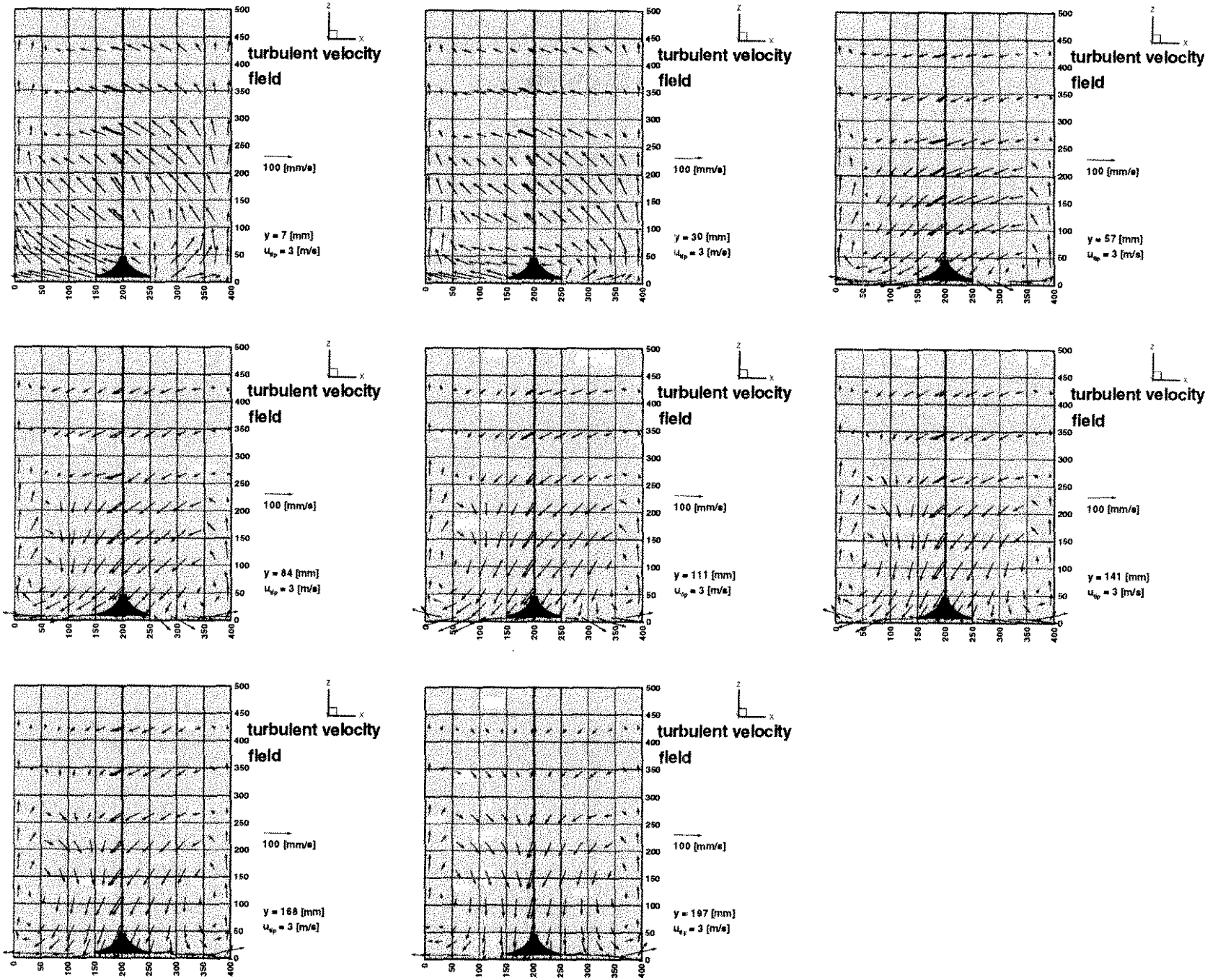

Fig. 9: Presentation of the vector field of velocity for the vertical planes

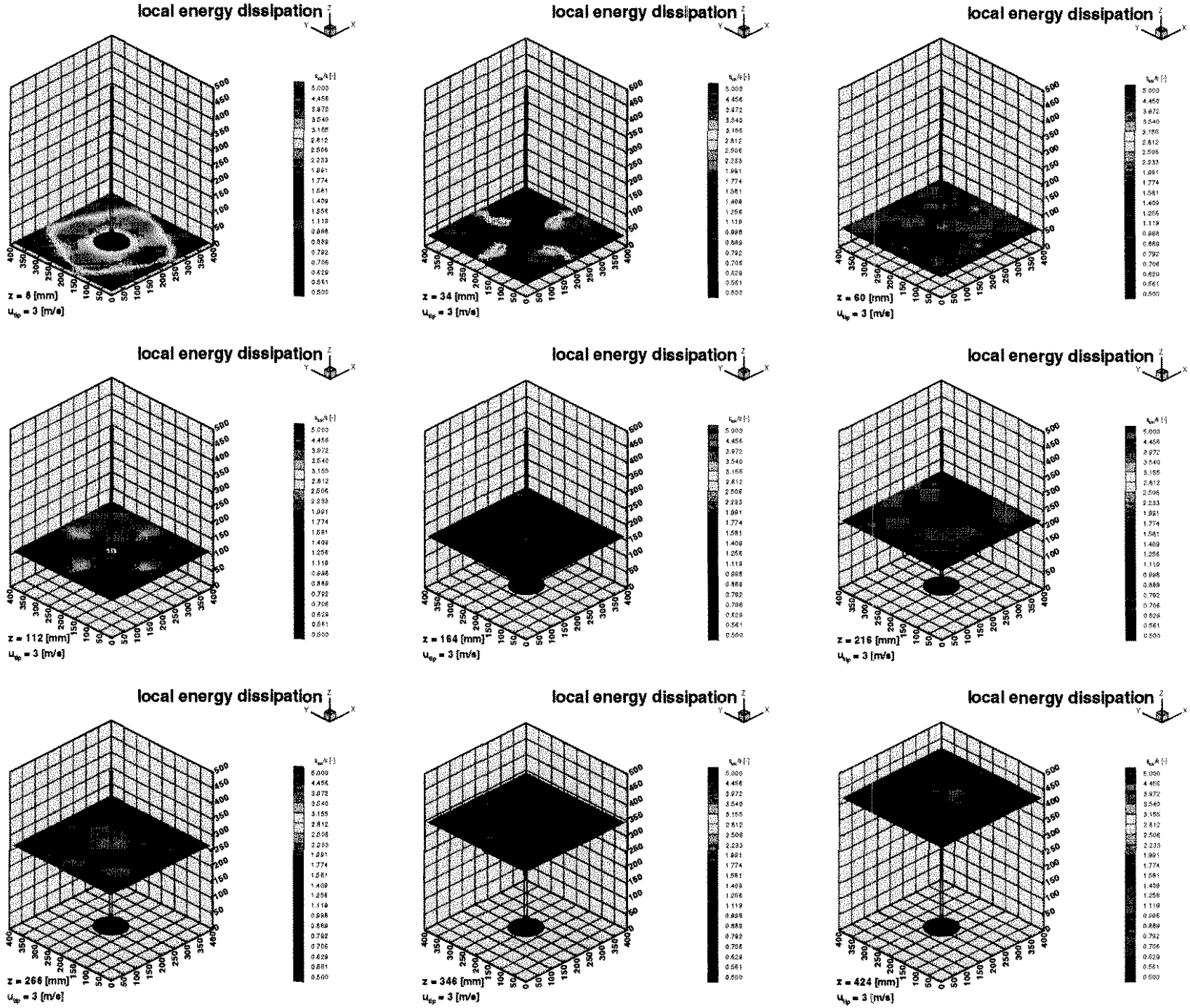

Fig. 10: Presentation of the local energy dissipation for the horizontal planes

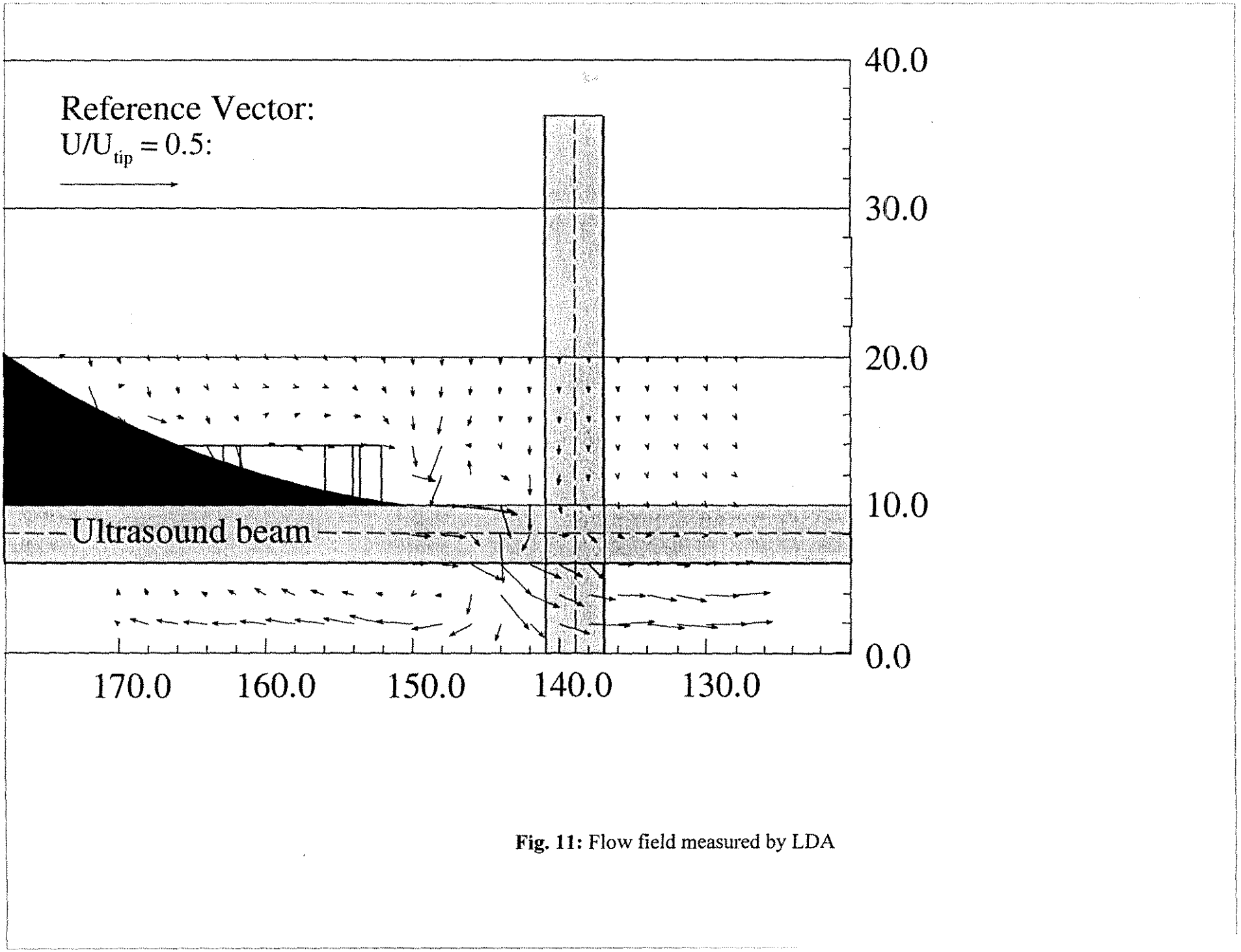

Fig. 11: Flow field measured by LDA

x-axis	7	30	57	84	111	141	168	197	-
y-axis	7	30	57	84	111	141	168	197	-
z-axis	8	34	60	112	164	216	268	346	424

Table 1: Coordinates of the measuring points in [mm] for the quadratic vessel

N	**20**	**50**	**100**	**200**
ε	±5,5 [mm/s]	±3,5 [mm/s]	±2,4 [mm/s]	±1,7 [mm/s]

Table 2: Number of measured values and statistical error

N	**20**	**50**	**100**	**200**
ε	±3,0 [%]	±1,9 [%]	±1,3 [%]	±0,9 [%]

Table 3: Number of measured values and relative error

Constant C	15.65
Micro scale (Taylor) λ	2.509 mm
Micro scale (Kolmogorov) η	0.143 mm

Table 4: Turbulence values for $L = d_R$